

Characterization of Deoxyribozymes that Synthesize Branched RNA

Yangming Wang and Scott K. Silverman*

Department of Chemistry, University of Illinois at Urbana-Champaign, 600 S. Mathews Ave., Urbana, Illinois 61801

Figures in this Supporting information are prefixed by the letter X (e.g., Figure X1) to distinguish them from those in the manuscript. All references cited by number are from the manuscript. See the manuscript's Experimental Section and refs. 6 and 9 for experimental details.

9F7 ligation assays with Zn^{2+} , Ni^{2+} , Co^{2+} , and Cd^{2+}

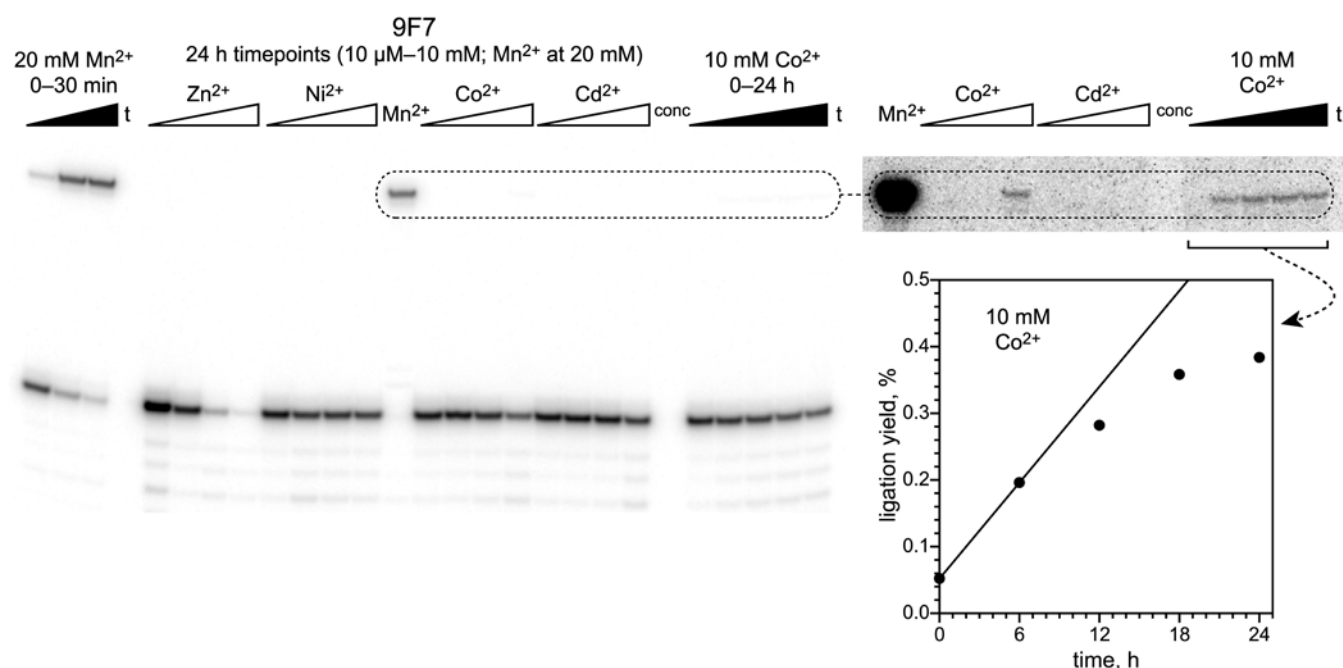


Figure X1. Assaying Zn^{2+} , Ni^{2+} , Co^{2+} , and Cd^{2+} for the ability to support ligation activity by 9F7. In the center portion of the gel image, the Mn^{2+} lane is a 24-h timepoint in 50 mM HEPES, pH 7.5, 150 mM NaCl, 2 mM KCl, and 20 mM $MnCl_2$ at 37 °C. For the other ions, 24-h timepoints are shown from similar reactions with 10 μM , 100 μM , 1 mM, or 10 mM of the particular ion (chloride salt) instead of Mn^{2+} . Degradation is evident with 10 mM Zn^{2+} ; there is significantly less degradation at shorter timepoints (e.g., 4 h; data not shown). On the far left are timepoints (0.5, 5, and 30 min) for 20 mM Mn^{2+} as a control reaction. On the far right is an experiment with 0-24 h timepoints for Co^{2+} (the darker image is 200 \times relative to the lighter image). Some loss of signal at the longer timepoints is apparent, because the intensity of the unligated band at 24 h is only 50% of the same band's intensity at the zero timepoint. This is probably via hydrolysis of the 5'- ^{32}P -monophosphate, because no generic degradation "ladder" is visible at any of the timepoints. The initial slope of the plot of ligation yield versus time is 0.024% per hour = $4 \times 10^{-6} \text{ min}^{-1}$, which is our best estimate of k_{obs} for Co^{2+} ; this is best described as an upper limit. With k_{obs} for Mn^{2+} of $\sim 0.3 \text{ min}^{-1}$, the relative rate for Co^{2+} is only about 10^{-5} that for Mn^{2+} . The left-hand substrate was ...UA \downarrow (uc) prepared by solid-phase synthesis. The purity of the $CoCl_2$ was 99.998% (Alfa). See below for similar data for 9F21.

9F21 ligation assays with Zn^{2+} , Ni^{2+} , Co^{2+} , and Cd^{2+}

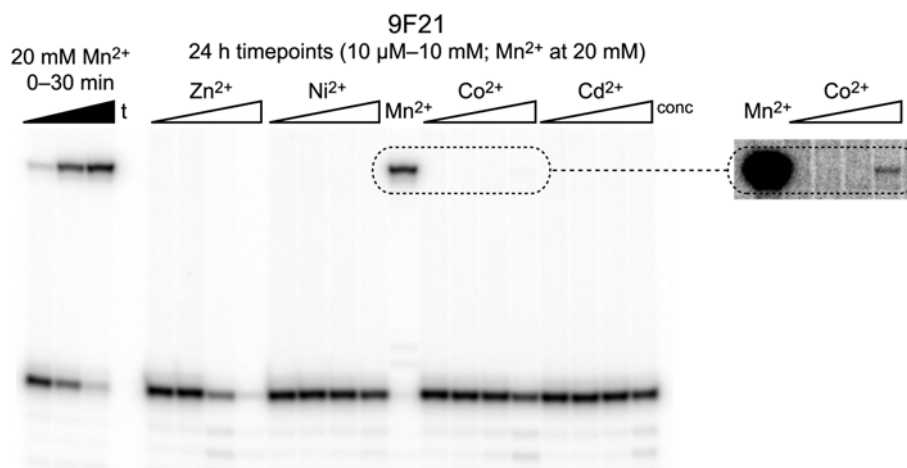


Figure X2. Assaying Zn^{2+} , Ni^{2+} , Co^{2+} , and Cd^{2+} for the ability to support ligation activity by 9F21. See Figure X1 for experimental details and similar results with 9F7.

Longer timepoints for 9F7 and 9F21 ligation assays with varying L substrate sequences

In Figure X3 are shown longer timepoints for the experiments of Figure 4, in which the first three nucleotides of the left-hand substrate RNA were varied. These positions includes the key branch-site nucleotide ... $CUA\downarrow(u)$. It is worthwhile to note that after 8 h incubation in 20 mM Mn^{2+} , conditions under which RNA degradation is not necessarily problematic, 9F7 can create 2',5'-branched RNA where the branch site is any of U, C, A, or G with potentially useful yields ($\geq 20\%$ in all cases).

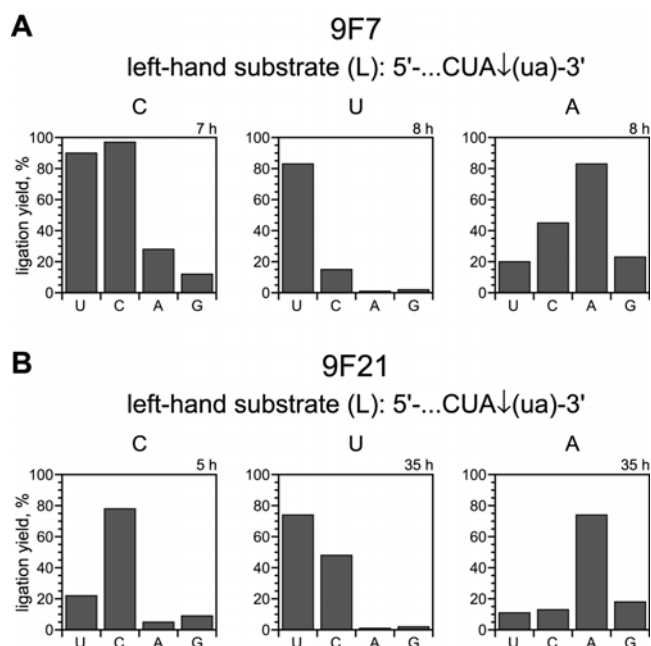


Figure X3. Longer timepoints for experiments of Figure 4 in which the $CUA\downarrow(u)$ nucleotides are altered. These six panels may be compared directly with the analogous panels in Figure 4, for which data were taken after 0.5 h incubation. See the Figure 4 caption for details of the experiments.

Testing $\text{NUA}\downarrow(\text{ua})$ and $\downarrow\text{GGAAN}$ positions for Watson-Crick base pairing

Assays similar to those in Figure 4 were performed for RNA substrates of sequence $\text{NUA}\downarrow(\text{ua})$ and (separately) $\downarrow\text{GGAAN}$ (Figure X4). These assays used 9F7 and 9F21 deoxyribozymes with all four possible DNA nucleotides (denoted Z) opposite the indicated RNA nucleotide (denoted X). Ligation yields are tabulated at short and long timepoints for each combination. The results show that Watson-Crick base pairs at these two positions support high ligation activity, with a pyrimidine (9F7) or C (9F21) required at the X position in the left-hand substrate (Figure 4) and a purine favored at the X position in the right-hand substrate (Figure 5). At the X–Z positions, mismatches generally but not always have reduced activity compared to Watson-Crick matches.

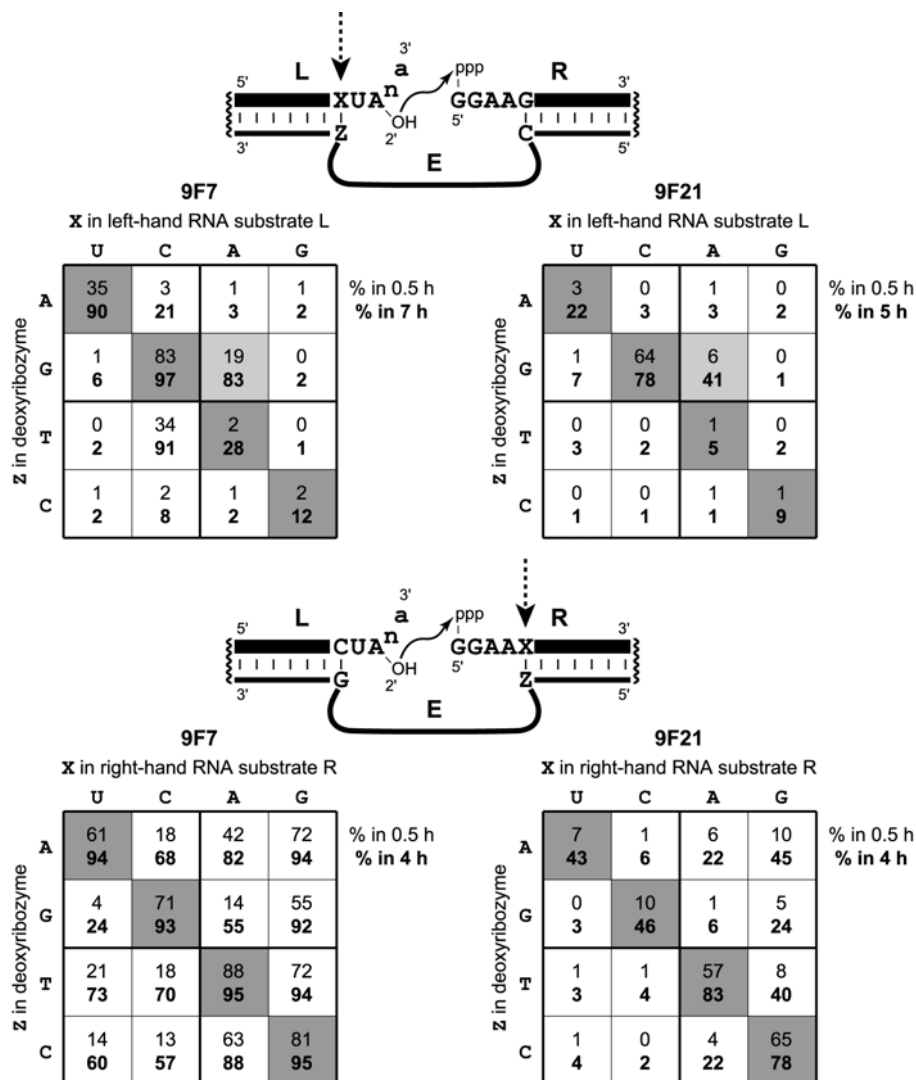


Figure X4. Testing for base pairing at two specific positions near the ligation site. For each of the 64 combinations of RNA substrates and deoxyribozyme (nucleotide X in RNA and nucleotide Z in DNA for the two positions in each of the two deoxyribozymes; $4 \times 4 \times 2 \times 2 = 64$), two timepoints were taken in addition to a 30-second timepoint. The first additional timepoint was at 0.5 h, and the second timepoint was at 4–7 h as indicated. The observed ligation yields at the two timepoints are shown in each box. Watson-Crick base pairs are shaded dark grey. The two A–G RNA–DNA combinations for the left-hand substrate for 9F7 and 9F21 are shaded light grey to highlight the anomaly that they provide higher ligation rate and yield than the Watson-Crick A–T combination.

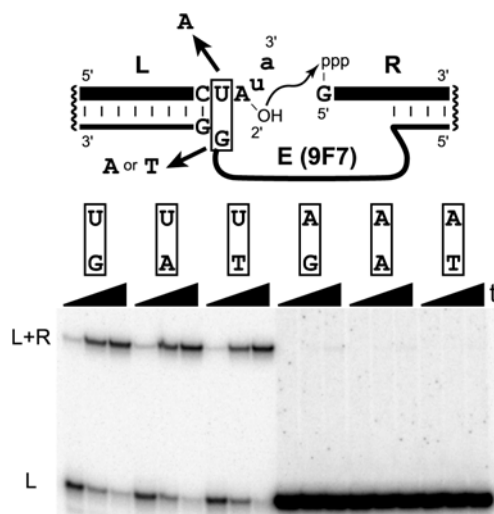
Testing a potential base-pairing interaction between the RNA and DNA in the left-hand binding arm

Figure X5. Testing for a Watson-Crick base pair between the left-hand RNA substrate nucleotide YUA↓ and the final nucleotide of the 9F7 enzyme region. The boxed RNA nucleotide was either maintained as U or changed to A, and the corresponding DNA nucleotide of 9F7 was changed from G to either A or T. The data indicate that a base pair is not formed between these two nucleotides. Assays were performed in 50 mM HEPES, pH 7.5, 150 mM NaCl, 2 mM KCl and 20 mM MnCl₂ at 37 °C. Timepoints were at 0.5, 5, and 30 min. The left-hand substrate was ...UA↓(ua) or ...AA↓(ua) prepared by transcription terminating with a 2',3'-diol.

Ligation by 9F7 to form linear 2'-5'-linked RNA using a short left-hand RNA substrate

The data in Figure 7 demonstrate that 9F7 and 9F21 each create linear RNA from a “tail-less” left-hand substrate. For the 9F7 product, whether the new ligation junction is 3'-5' or 2'-5' was distinguished using the two complementary assays shown in Figure X6. These assays were described in detail in our previous manuscript (ref. 6). Briefly, an appropriate 8-17 deoxyribozyme selectively cleaves at the newly created A↓G junction if the linkage is 3'-5' (but not 2'-5'), whereas 100 mM Mg²⁺ promotes selective cleavage of an RNA 2'-5' linkage (but not a 3'-5' linkage) at pH 9 in the presence of the exactly complementary DNA. The results in Figure X6 for the 9F7 tail-less ligation product unambiguously indicate that this product is 2'-5'-linked, consistent with our initial expectation. This product is formed by reaction of the same adenosine 2'-hydroxyl that reacts when the left-hand RNA substrate has a 3'-tail of any length greater than zero (i.e., when the adenosine 3'-hydroxyl is already participating in a conventional phosphodiester bond). Therefore, these data show that removing the 3'-tail does not change the site of reactivity, but this does lower the ligation rate considerably (compare Figures 9 and 10).

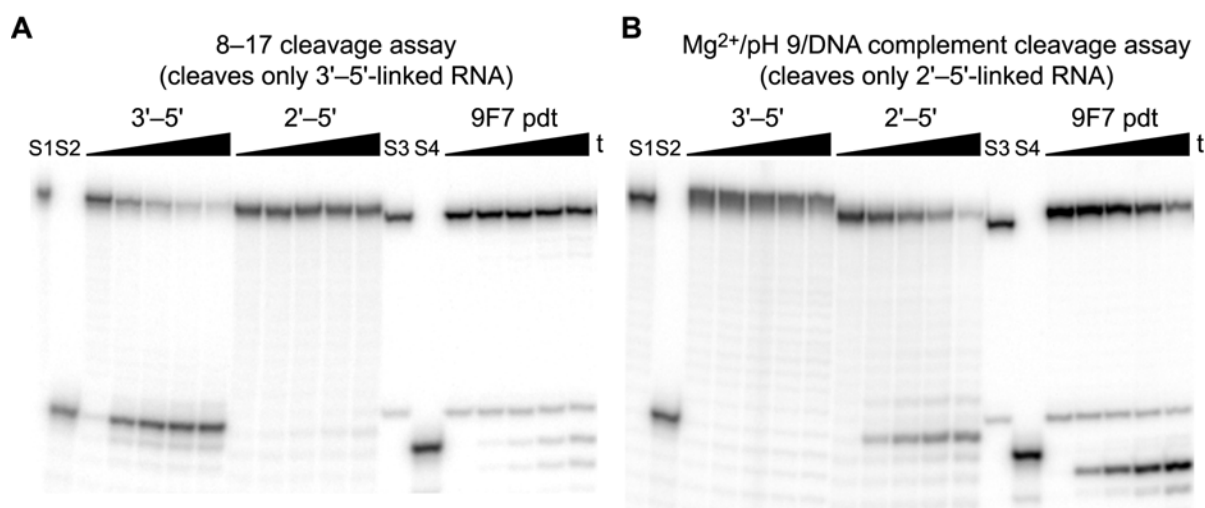


Figure X6. Assays to distinguish the 3'-5' versus 2'-5' nature of the linear 9F7 ligation product from the tail-less left-hand substrate. Both of these assays are described fully in ref. 6. (A) Using the 8-17 deoxyribozyme to reveal 3'-5' linkages. Timepoints at 0, 20 min, 1, 3, and 6 h. S1 is the 3'-5'-linked standard RNA from ref. 6 that is made from a left-hand substrate 2 nt longer than the tail-less substrate. S2 is the left-hand substrate standard ...UAUA terminating with a 2',3'-cyclic phosphate (i.e., the expected product from 8-17 cleavage of S1). S3 is the standard for the untreated 5'-³²P-radiolabeled 9F7 ligation product. S4 is the 5'-³²P-radiolabeled tail-less left-hand RNA substrate standard. The timepoints marked 3'-5' show the expected cleavage of the 3'-5'-linked standard RNA by 8-17, whereas the timepoints marked 2'-5' show the expected lack of cleavage of the 2'-5'-linked standard RNA. The 9F7 ligation product shows essentially no cleavage by 8-17 (<5%; comparable to Figure 3C of ref. 6). The trace impurity (lower band) in S3 and the 9F7 pdt lanes is not identified. (B) Using 100 mM Mg²⁺ at pH 9 in the presence of the exactly complementary DNA to reveal 2'-5' linkages. Timepoints at 0, 2, 6, 12, and 24 h. Standards S1-S4 as in panel A. Note that S4 migrates slightly slower than the 9F7 pdt cleavage product as expected, because S4 has a 2',3'-diol terminus whereas the cleavage product has a 2',3'-cyclic phosphate. The 9F7 ligation product shows the expected cleavage for a 2'-5' linkage with $t_{1/2} \approx 11$ h (ref. 6).

9F21 is more sensitive than 9F7 to the left-hand substrate 3'-tail length

The data in Figure 8 demonstrate that 9F7 tolerates increasing the 3'-tail length with no reduction in yield and only a two-fold decrease in k_{obs} . Here we show that 9F21 is more sensitive than 9F7 to the tail length. When the same set of left-hand substrates as in Figure 8 was tested with 9F21, the k_{obs} was considerably lower for the longer substrates (Figure X7). While the k_{obs} decreases by ~ 40 -fold when the tail length is increased from 2 to 8 or 20 nt, the k_{obs} is comparable ($\sim 0.003 \text{ min}^{-1}$) for both of the longer tail lengths. This suggests that 9F21 will accept even longer 3'-tails on left-hand RNA substrates.

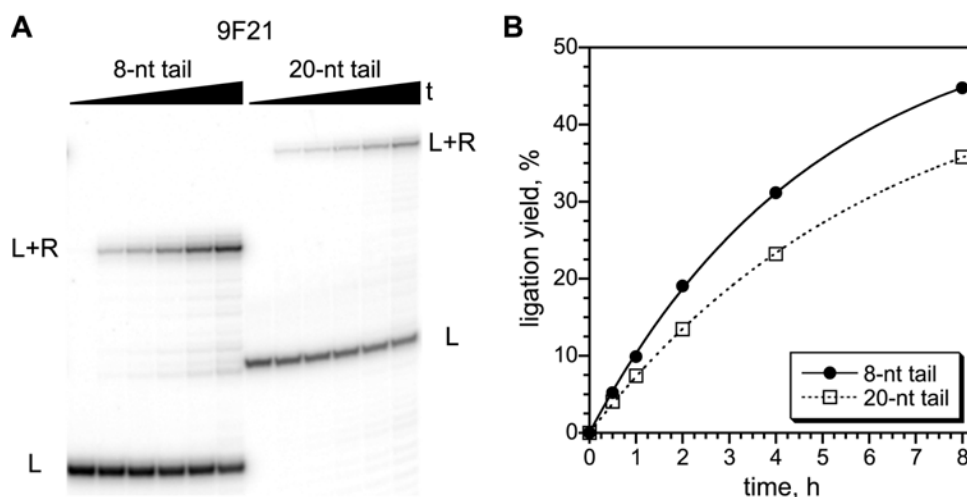


Figure X7. Testing 9F21 with longer left-hand RNA substrates. The experiment is essentially the same as that of Figure 8, with 9F21 instead of 9F7. (A) Gel image. (B) Kinetics plot. k_{obs} values: 8-nt tail, 0.0034 min^{-1} ; 20-nt tail, 0.0026 min^{-1} . See Figure 1C for 9F21 with a 2-nt tail ($k_{\text{obs}} = 0.13 \text{ min}^{-1}$).